Applied Magnetic Resonance 2, 29–60 (1991)

Applied Magnetic Resonance

Investigation of Biological Systems by High Resolution 2 mm Wave Band ESR

V.I.Krinichnyi

Department of Kinetic and Cathalysis, Institute of Chemical Physics of the Academy of Sciences of the USSR, Chernogolovka, USSR

Received November 23, 1990

Abstract. The application of the high resolution ESR technique for investigation of various biological systems is shown. The advantages of the technique in the study of structural, conformational and dynamic characteristics are exemplified by spin labeled human serum albumin, egg lysozyme, liposome membranes, inverted micelles, α-chymotrypsin, cotton fiber and cellulose. The polarity of microenvironment and the mechanisms of molecular mobility of the objects under study are determined. The combination of high resolution and saturation transfer techniques is shown to give the detailed analysis of very slow molecular motions in biological objects. Peroxide radicals in biosystems are identified by the ESR spectra of the 2 mm wave band.

1. Introduction

Various methods exploiting labels or probes are widely used in investigations of structure and dynamics of biological systems. They include luminescent labels [1], nuclear gamma-resonance (NGR) labels [2], electron scattering labels [3] and others. One of the most commonly used is the spin label and probe method based on the introduction of a nitroxyl radical into biological systems [4–7]. The ESR spectral parameters of radicals depend on the polarity, structure and dynamics of the microenvironment in the place of their localization. Therefore, an introduction of spin labels or probes into various sites of enzymes, nucleic acids and membranes reveals the profiles of polarity and molecular mobility of the systems under study and their topography.

Such investigations are most commonly carried out in the 3 cm wave band ESR. However, the ESR spectra of organic free radicals are registered in a narrow range of magnetic fields at this radio frequncy (RF) wave band. This

leads to a poor resolution of multicomponent ESR spectra and makes difficult the application of this method to the study of structure and dynamics of microenvironment in biological systems.

For example, the 3 cm wave band ESR spectra do not give an unequivocal interpretation of reasons for changes caused by relaxation in the spectrum (e.g., slow anisotropic movement of radicals in the frequency range $\nu = 10^7 - 5 \cdot 10^8$ s^{-1} [4] or fast rotation of a nitroxyl radical with 10^9 s^{-1} frequency within a cone [8]). A few additional difficulties arise when registering ESR spectra of some paramagnetic centers with similar magnetic parameters, as well as when determining micropolarity in biological systems [6].

Thus the ESR study of biological systems at the 3 cm wave band faces considerable limitations.

In some specific cases the increase in the method accuracy is achieved by a non-modulation registration of ESR spectra [9]. Low molecular mobility in the frequency range of $\nu < 10^7$ s^{-1} can be registered using microwave saturation transfer (ST ESR) [5,10]. The efficiency of the 3 cm wave band technique may be increased by deuteration of radicals and molecules of medium, which lower the contribution of their protons to the width of the spectrum components [11].

However the ESR technique in millimeter wave band proved to be a more efficient and precise method of spectra registration [11–16]. In this region the absolute sensitivity and spectral resolution for polyoriented paramagnetic centers in model systems increased considerably.

The present paper reviews first results obtained in the study of microstructure and dynamics of a wide range of biological samples (proteins, enzymes, membranes, micelles, α-chymotrypsin, cotton fibers and cellulose) using a high spectral resolution ESR at the 2 mm wave band [17]. The potential advantages of this technique in the detailed study of very slow anisotropic movements of nitroxyl radicals by ST ESR and in the identification of peroxide radicals in biological systems are shown.

2. The ESR Method in the Study of Biological Systems

Paramagnetic properties of nitroxyl radicals used as spin labels and probes are due to the intrinsic magnetic momentum of the unpaired electron localized on the molecular p-orbital (Fig.1a). When the external magnetic field H_0 is applied to a system of such radicals, their spins are oriented along or opposite to the field direction. These orientations are characterized by the different value of interaction with the magnetic field, therefore in the paramagnetic system there appear two Zeeman energy levels with different spin population. If besides the constant magnetic field the spin system interacts

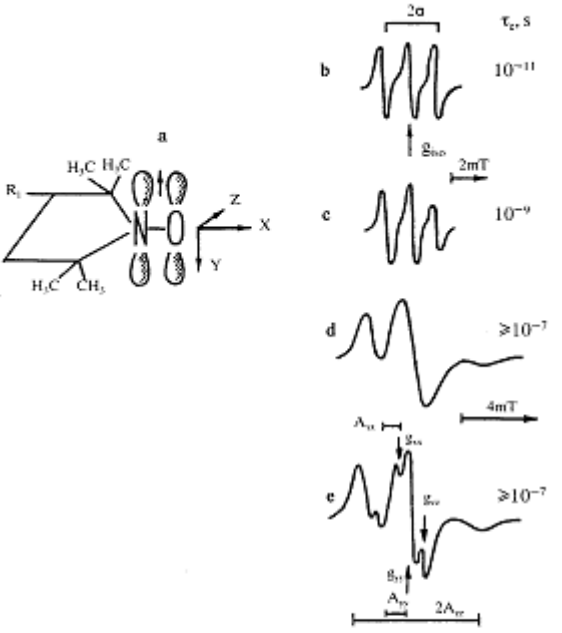

Fig.1. a Electronic configuration of the nitroxyl radical in the molecular system of coordinates (R is the radical substituent). b–d Typical ESR spectra of this radical at various correlation times of rotation and e of a deuterosubstituted radical in d_8-toluene at 140 K [6,50]. The measured magnetic parameters are shown too.

with the RF field of the ν frequency and H_1 magnetic component which is perpendicular to H_0, an induced transition from one spin state to another one with the resonant absorption of the RF energy will take place. This is true for the condition:

$$h\nu = g\beta H_0 , \tag{1}$$

where h is the Plank constant, ν is the frequency of RF field, g is the Lande factor equal to 2.00232 for a free electron, β is the Bohr magneton and H_0 is the strength of the external magnetic field.

Atomic orbits of the nitroxyl radical are rigidly fixed and oriented in the molecular system of coordinates by strong atom electric fields. Besides, the unpaired electron participates in the orbital motion around O and N heteroatoms, which gives rise to a considerable deviation of its g-factor from the purely spin one and its dependence on the radical orientation in the magnetic field.

The g-factor differences from the 2.00232 value at the magnetic field along the molecular x- and y-axes will constitute [18]:

$$\Delta g_{xx} = g_e \lambda_0 \varrho_0^2 / \Delta E_{xx^*} \quad \text{and} \quad \Delta g_{yy} = g_e \lambda_0 \varrho_0 / \Delta E_{xx^*} \tag{2}$$

respectively, where g_e is the g-factor of free electron; λ_0 is the constant of spin-orbital interaction with oxygen nucleus; ϱ_0^2 is the density of the unpaired electron on the oxygen atom; ΔE_{xx^*} and ΔE_{xx^*} are energy differences of the corresponding molecular orbitals. The weakest change in the g-factor is observed at the magnetic field along z-axis of the radical.

The other important characteristics of a nitroxyl radical is the value of hyperfine interaction (HFI) of the unpaired electron with the nuclear spin ($I=1$) of a nitrogen atom. This interaction depends on the configuration and density of a spin cloud on the nitrogen nucleus and is characterized by A-tensor.

Thus the magnetic parameters of a nitroxyl radical are affected by its orientation in the magnetic field and defined by g- and A-tensors.

In the condensed media with low viscosity the components of g- and A-tensors are averaged due to a fast radical rotation. In this case the ESR spectrum of the nitroxyl radical is a triplet of equidistant lines with equal intensity; it is characterized by the isotropic magnetic parameters (Fig.1b):

$$g_{iso} = (g_{xx} + g_{yy} + g_{zz})/3 \quad \text{and} \quad a = (A_{xx} + A_{yy} + A_{zz})/3\,, \tag{3}$$

where g_{ii} and A_{ii} are the principal values of g- and A-tensors, respectively. With the increase in the medium viscosity the anisotropy of the radical magnetic parameters is registered in ESR spectra (Figs.1c–1e).

The magnetic parameters are essentially affected by structural and dynamic properties of the nitroxyl radical environment.

In biological systems nitroxyl radicals can form donor-acceptor, electrostatic and other complexes with the molecules of environment [19]. About 1% spin density in donor-acceptor complexes is transferred to the ligand as a result of a hydrogen bond formation. The magnetic constants of such a complex depend on the donor-acceptor properties of the ligand. In electrostatic complexes the interaction between the dipoles of the ligand and the radical

causes electrostatic perturbation of Hückel molecular orbitals and Coulomb integral of the N—O fragments. The dipole-dipole interaction leads predominantly to the changes in the A_{zz} value of the HFI tensor [20], which can be determined from the following formula:

$$\delta A_{zz} = B\mu_1 \varrho_1 M_1^{-1}, \tag{4}$$

where $B = 22er\beta^{-1}kT\mu_r$ (e is the elementary charge, r is the N—O-fragment radius, β is the resonant integral of the C—C-bond, k is the Boltzmann constant, T is the absolute temperature, μ_r is the radical dipole momentum), ϱ_1, M_1 and μ_1 are the efficient density, the molecular weight and the dipole momentum of the environment, respectively.

The complex formation also leads to a shift of the n—π^*-band in its electron absorption spectra, that is an evidence for the energy change in the n—π^* orbital transition. The radical interaction with the electron acceptor and electron donor ligands lowers the energy levels of n- and π^*-orbitals, respectively, thus affecting the g_{xx} value [18].

Thus in the condensed media the increase in the polarity of the nitroxyl radical microenvironment leads to the decrease of g_{xx} value and to the increase of A_{zz} value. Unlike simple models, in biological systems there occurs a formation of radical complexes with environmental hydroxyl groups of different nature. It can cause the inhomogeneous broadening and sometimes the splitting of separate components of the ESR spectrum.

As stated above, the increase in viscosity results in the decrease of the radical rotation frequency, and the anisotropy of its magnetic parameters appears in ESR spectra (Figs.1c—1e). The theory of spectra of isotropically rotating radicals with the correlation time of $\tau_c < 10^{-9}$ s is developed in [21—23]. At a slower rotation it is usually necessary to carry out the comparison between the experimental and computed ESR spectra. The computation algorithm and the shape of the computed ESR spectra depend on the motion pattern chosen. As a rule, the mobility of spin labels and probes in biological systems is determined by the various parameters of their environment and is strongly hindered. Because of the non-sphericity of regularly used radicals their motion is generally anisotropic in the majority of biological systems. In this case the changes caused by relaxation in the ESR spectra of randomly oriented spin-labeled systems should not appear for that part of radicals whose preferable rotation axes are mainly oriented along the field.

Thus for a radical with a preferable rotation around the molecular x-axis the changes caused by relaxation take place primarily for y- and z-components of the ESR spectrum as the motion is intensified. At further development of the process the x-component is also involved in it. The changes caused by relaxation manifest in the shift and broadening of the components of the

ESR spectrum. The value of broadening δH_i is proportional to frequency of slow ($\nu < 5 \cdot 10^8$ s^{-1}) radical reorientation with respect to the direction of the external magnetic field [15]:

$$\delta H_x = 2\nu_\perp / \gamma, \qquad \delta H_y = \delta H_z = (\nu_\perp + \nu_\parallel)/\gamma, \tag{5}$$

where γ is a hyromagnetic ratio, $\nu_\parallel$ and $\nu_\perp$ are the frequencies of the radical reorientation in parallel and perpendicular orientation to the external field, respectively. These conclusions are also valid for the radical with other axes of the preferable rotation.

Thus the precise study of the structure and dynamics of the biological spin-labeled systems requires the registration of all principal values of their magnetic constants.

However, there is an almost complete overlapping of all the lines in the ESR spectrum of nitroxyl radical in condensed medium registered at the 3 cm wave band (see Figs.1d and 1e). Some of the components of g- and A-tensors of deuterated spin systems may be defined from the ESR spectra of the 3 cm wave band because of smaller line width (Fig.1e). In real biological systems the problem of the definition of the magnetic parameters is more complicated. As a rule, only magnetic parameters of g_{zz}, A_{zz} and the z-component width are determined from the 3 cm ESR spectra.

As stated above, the ESR method is more accurate and informative at a higher registration frequency. However, at the 8 mm ESR wave band the anisotropy of the g-factor is comparable with that of HFI so that overlapping of lines of different canonical orientations retain to a considerable degree [24].

At the 2 mm wave band the resolution between spectral lines increases by more than an order of magnitude [13] (Fig.2), that makes it possible to determine all magnetic parameters of nitroxyl radicals. An independent analysis of changes caused by relaxation in each component of the spectra and the anisotropic low molecular rotations study become possible. Though the A_{xx} and A_{yy} values are not resolved in biological systems because of the interaction of unpaired electron with radical protons and its environment, they are easily determined from the halfwidth of the corresponding canonical components.

Thus, high spectral resolution at the 2 mm wave band of ESR allows to study fine structural and conformational transitions in native biological object. At this wave band the configuration of the spin distribution in the organic radicals can be more successfully determined and the registration of several radicals with similar magnetic parameters can be carried out as well.

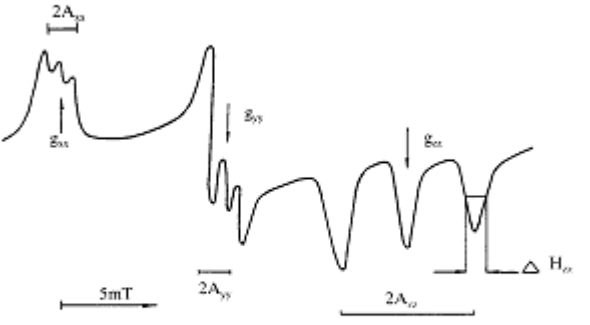

Fig.2. The ESR spectra of the 2 mm range of the deuterosubstituted nitroxyl radical in d_8-toluene registered at 140 K [50]. The measured magnetic parameters are shown.

3. Peculiarities of the 2 mm ESR Spectroscopy

According to Eq.(1), microwave radiation at 2 mm wavelength and a strong constant magnetic field (about 5 T) are required for the registration of paramagnetic centers with $g \simeq 2$ at 2 mm ESR wave band. Therefore the 2 mm wave band ESR spectrometer includes an H_{011} microwave cavity and a super conducting magnet [25].

The general sketch of the 2 mm wave band ESR device is given in Fig.3.

The main part of the spectrometer includes the microwave klystron oscillator (11) with some elements of the wave guide section and a cryostat (1) with a super conducting solenoid (2), in whose warm channel the tunable resonator (5) with a sample (6), temperature-sensitive (3) and modulator (4) coils are inserted. A sample in a thin (0.5 mm) quartz capillary (7 mm long) is put into the center of the cavity with the mobile plunger.

The microwave cavity with the sample inside is temperature-controlled (80–370 K). However, the registration of the ESR spectrum at lower temperatures is also available.

The Q-factor of the cavity (inner diameter 3.5 mm, operation height 1.5 mm) is equal to 2000. The value of a microwave field magnetic component H_1 is equal to 20 μT in the center of the cavity. The magnetic field inhomogeneity in the sample situation does not exceed 10^{-5} T/mm.

The absolute point-sample sensitivity of the spectrometer is $5 \cdot 10^8$ spin/mT. The concentration sensitivity for an aqueous samples is $6 \cdot 10^{13}$ spin/mT

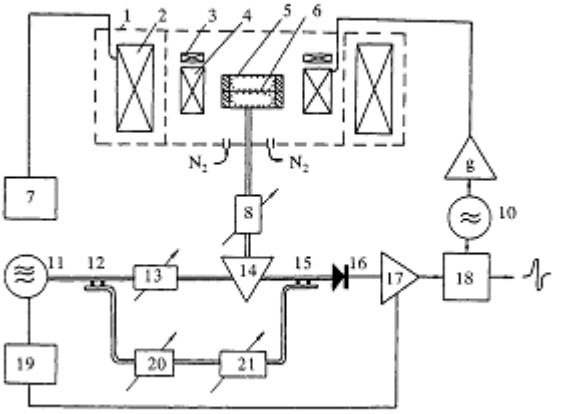

Fig.3. The sketch of the 2 mm wave band ESR spectrometer [25]: 1 – helium cryostat, 2 – superconducting solenoid, 3 – temperature-sensitive coil, 4 – ac modulator coil, 5 – microwave cavity, 6 – sample, 7 – solenoid supply, 8 and 21 – phase shifter, 9 – ac modulator amplifier, 10 – ac oscillator, 11 – klystron oscillator, 12 and 15 – directional MW couplers, 13 and 20 – MW attenuators, 14 – MW circulator, 16 – super low temperature (4.2 K) barretter, 17 – ac preamplifier, 18 – ESR amplifier and synchronous detector, 19 – section of auto adjustment of the MW klystron oscillator.

cm^3. In the latter case the samples were placed to capillaries of smaller diameter to retain high Q-factor.

All experiments were carried out with the high frequency (100 kHz) modulation.

The g-factor calibration is performed using the Mn^{2+} standard with a=8.74 mT and g=2.00102. The second order correction to the effective resonant field [26] for this standard is 65 μT. This does not add an essential error to the determined magnetic constants.

4. The Structure of Microenvironment and Molecular Mobility of Nitroxyl Radicals in Biological Systems

In the ESR investigation of biological objects at the 2 mm wave band the following nitroxyl radicals were used as spin labels and probes:

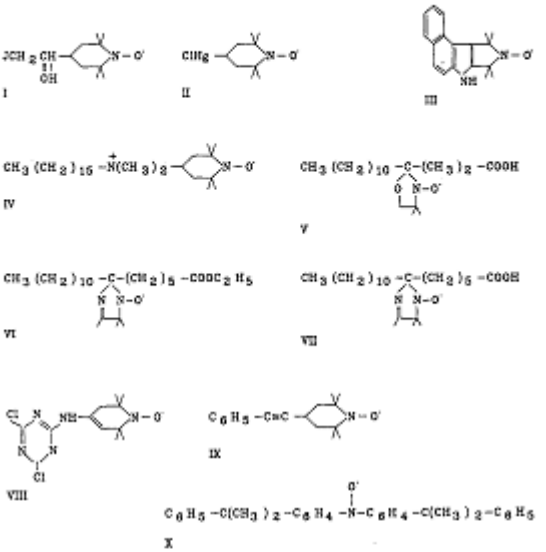

Magnetic constants of the spin labels and probes in various matrices were determined from the ESR spectra registered at the temperature when all the movements in the sample are frozen (see Appendix).

Let us consider the influence of the radical structure on its ability to form complex with microenvironment. Unlike the five-member radicals with a flat head, the six-member radicals are characterized by a chairwise form of the head, therefore the six-member radicals probably possess the higher accessibility of their n-orbital for the partners and consequently higher energy of the hydrogen bond with them.

In fact, the average slopes of the correlation dependence between g_{xx} and A_{zz} of six- (I,II) and five-member (III,VII,VIII) radicals in biological and model systems are $2.3 \cdot 10^{-3}$ mT^{-1} and $1.2 \cdot 10^{-3}$ mT^{-1}, respectively (see Appendix). This confirms a greater shift of the spin density to the nitrogen atom in the six-member radicals in their complex formation with the microenvironment of the same polarity [18].

The correlations between experimental changes of A_{zz}, $\delta A_{zz}^{\exp}$, and calculated ones, $\delta A_{zz}^{\text{calc}}$, for six-member radical I (dots) and for five-member radical VII

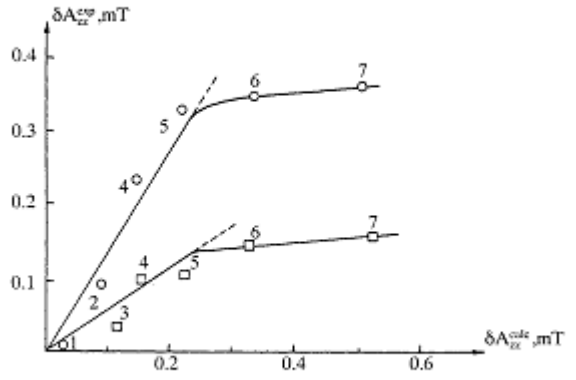

Fig.4. The correlation plots δA_{zz}^{exp} vs. δA_{zz}^{calc} for radicals I (circles) and VII (squares) in frozen toluene (1), isopropanol (2), n-propanol (3), ethanol (4), methanol (5), water-ethanol (3:1) mixture (6) and water-glycerol (10:1) mixture (7) [17].

(squares) in various model systems are given in Fig.4. As seen from Fig.4, the linear dependence between the δA_{zz}^{exp} and δA_{zz}^{calc} values for both radicals retains only in model systems with the dipole momentum not higher than 1.7 D. Therefore, the presence of both electrostatic and donor-acceptor radical complexes with the microenvironment may be assumed for these systems. The different slope shows higher sensitivity of six-member radicals to the polarity and structure of their environment.

Thus, a simultaneous existence of different radical complexes is possible both in model and biological systems. The magnetic constants of the radical are determined by the proportion between these complexes, the efficient polarity and structure of its environment.

As shown above, the g_{xx} and A_{zz} values are most sensitive to the changes in the polarity and the structure of the nitroxyl radical environment. Therefore, these properties are determined using the correlation between these values, g_{xx} and A_{zz}, in biological and model systems.

Egg lysozyme. Lysozyme samples modified by spin label I on Hys-15 group as described in [27] were studied at 2 mm wave band ESR [28]. The ESR spectrum of the lyophilized sample is characterized by a strong inhomogeneous broadening of the canonical components. The broadening is partially decreased after sample damping. This fact shows that the interaction between nitroxyl radicals and hydroxyl fragments is of different nature in the dry sample.

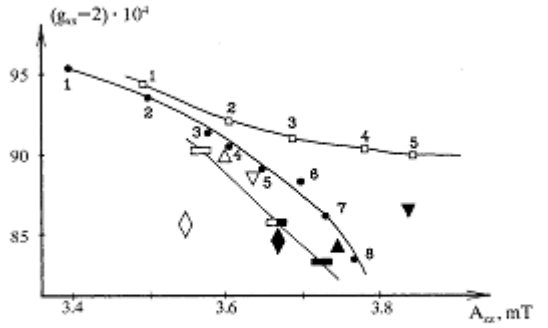

Fig.5. The correlation plot (g_{xx} and A_{zz}) for radical I in frozen (140 K) (painted circles) toluene (1), isobutanol (2), ethanol (3), water-ethanol mixture with 0.25 (4), 0.50 (5), 0.66 (6) H_2O content, methanol (7), water-glycerol (10:1) mixture (8), egg lysozyme (squares) of the 0.04 (1), 0.35 (2), 0.60 (3), 0.80 (4), 0.96 (5) relative humidity degree, *R*, human serum albumin (triangles up) of the 0.04 (open) and 0.96 (painted) relative humidity degree, α-chymotrypsin (rectangles) of the 0.04 (open), 0.65 (semipainted) and 0.96 (painted) relative humidity degree, radicals II (triangles down) and III (rhombuses) in the human serum albumin of the 0.04 (open) and 0.96 (painted) value of relative humidity degree [28,30].

The magnetic parameters of the frozen egg lysozyme, α-chymotrypsin samples modified by radical I, the human serum albumin samples modified by radical I–III of same relative humidities and solution of radical I in organic solvents of different polarity are presented in Fig.5. As seen from Fig.5, the increase in the polarity of the microenvironment of radical I in model systems causes gradual decrease in the g_{xx} and increase in the A_{zz} values. This fact shows unequivocally the formation of an $n-\sigma$ radical complex with molecules of the medium [19]. The deviation of the experimental correlation between g_{xx} and A_{zz} from linearity can be explained by the presence of electrostatic and donor-acceptor complexes in model systems.

A gradual change in the magnetic constants of label I takes place at the lysozyme saturation by water (see Fig.5). Obviously, there exists an $n-\sigma$ complex of the radical N–O fragment with the environment in modified lysozyme. The close values of magnetic constants of the radical I in lyophilized protein and in the butanol model system enable to suppose the similar polarity and structure of the radical fragment environment in these matrices.

The deviation of the correlation between g_{xx} and A_{zz} from that for model systems may be explained by the conformational changes in the radical structure under the action of protein media.

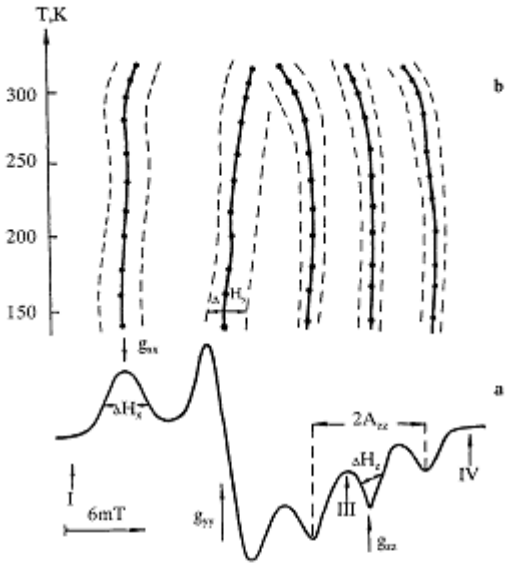

Fig.6. a The ESR spectra of radical I in egg lysozyme with the value of relative humidity degree of 0.96 registered at 130 K at the 2 mm wave band and b the plot of the position (solid curve) and half-width (dotted curve) of the ESR spectrum components vs. temperature [28]. I, III, IV – the positions of Mn^{2+} standard components.

The changes caused by relaxation in the ESR spectra of spin-labeled samples were not observed at humidity less than 0.8 in the 130–320 K temperature range. It can be explained by the rigid fixing of the radical fragment by nearest H-containing groups of protein.

Heating of the water-saturated sample results in the considerable reversible broadening and a shift of the principal components of the ESR spectrum (Fig.6b). In the 130–320 K temperature range the narrowing of the *x*-component of the spectrum is observed due to the averaging of the unresolved hyperfine structure (HFS) of radical and protein fragment protons. It is an evidence of the moistening effect on the molecular mobility in the sample even at low temperature (T<200 K). At temperatures higher than 250 K the *x*-component of the ESR spectrum is shifted to low fields. It cannot be explained by an increase of the molecular mobility. Since there was no such an

effect in the lyophilized sample, it can be assigned to the weakening of the hydrogen bond in the N—O fragment with the water molecules in the vicinity.

The changes caused by relaxation in the other components of the ESR spectrum of the water-saturated sample are registered above 260 K and can be explained by anisotropic rotational diffusion. It is probably caused by weakening of the interaction between the radical N—O fragment and the surface protein groups and further hydration of the radical and protein groups. In this case, the water molecules appear to be specific plasticizers of the protein globule mobility which in turn promotes the radical rotation.

In the case of anisotropic motion the broadening and the shift of the principal values are different for canonical components of the ESR spectrum. In the ESR spectrum of spin-labeled lysozyme the y-component is broader than the other ones because of the weak anisotropy of the radical rotation around the z-axis. The theoretical calculation made by Antsiferova [28] confirmed this supposition.

According to the NMR data [29], the nitroxyl fragment of the label I is 11 Å far from the Hys-15 NH-group and 10—11 Å far from the Phe-3, Val-92 and Uso-88 protons. It corresponds to the stretched conformation of the label and the localization of its nitroxyl fragment near a hollow formed by the mentioned hydrophobic groups. The rotational diffusion of the nitroxyl fragment remains slow, $\tau_c \geq 5 \cdot 10^{-8}$ s ($\tau_\perp \geq 1.1 \cdot 10^{-7}$ s, $\tau_\parallel \geq 2.2 \cdot 10^{-8}$ s), up to 305 K. The rotation is likely to occur around the —C—NH— and $-CN_2CO-$ bonds, whose direction is close to the z-axis of the radical g-tensor. The mobility is limited by the interaction of the radical with the protein groups and perhaps with the molecules of "viscous" water, close to the protein surface. The mobility depends on the microviscosity of the water-protein matrix in label vicinity. The efficient local viscosity in the hydrophobic pocket of lysozyme is ca 60 Pa s, as calculated according to Stokes-Einstein equation at 300 K from 2 mm band spectra.

Human Serum Albumin (HSA). The HSA samples labeled by radicals I—III were studied in [30]. The modification of SH-groups of HSA by radicals I and II and the insertion of hydrophobic probe III were carried out as described in [31].

The magnetic constants of the HSA modified by these radicals (relative humidities were 0.04 and 0.96) are presented in Fig.5.

The magnetic constants of the HSA modified by radicals I and II (humidity 0.04) fall within the correlation between g_{xx} and A_{zz} for model systems, which evidences for the similarity of structures and polarities of the microenvironment of these labels in lyophilized HSA sample and in frozen ethanol system. The analysis of changes in the magnetic parameters of radicals II and III in model systems is required for the study of the influence of their structure and polarity on the microenvironment in HSA.

The ESR spectrum of HSA modified by label II contains split x-component due to the different types of interaction between radicals and environment in this system.

At the increased humidity the radical fragment of label I is solvated by the water molecules similarly to the water-glycerol mixture. Label I in HSA seems to be accessible to water environment. Apparently, the same picture of properties is characteristic for water-saturated HSA and other radicals. However, various interactions of radicals I and II with the microenvironment may be proposed for water-saturated HSA.

Liposome Membranes. Conformational and molecular dynamic properties of phospholipid bilayers are of extreme importance in the realization of biochemical and biophysical processes in membranes.

The comparison of molecular mobility of probes IV and V introduced into the aqueous solution of phosphatidylcholine liposomes in the phosphate buffer (pH 0.7; 0.02 M) and the molecular mobility of probe VI in the ethanol matrix was made in [32]. At 180 K the shape of the ESR spectra of the liposome membranes with the probes inserted differs only slightly from those of the frozen ethanol matrix. In the latter model system at $T \lesssim 160$ K the splitting of the x-component of the spectrum was observed which could be explained by the presence of several types of radical complexes with the solvent molecules.

The heating of the studied systems leads to the appearance of the changes caused by relaxation in lineshape of their spectrum. The temperature-dependent changes in the width and the position of the ESR spectra components of biological and model systems are illustrated by Fig.7.

As seen from Fig.7c, the isotropic rotation of the radical VI is observed in the ethanol matrix at $T > 150$ K. A different mode of the changes in the line shape is observed for the membrane systems (Figs.7a and 7b) The main difference from the model system (besides the shift into the region of higher temperatures and weaker changes) is the noticeable shift of the x- and z-components at their weak broadening. These differences can be explained by the weak anisotropic rotation of the radical around the y-axis or by the decrease in the contribution to the line width of the unresolved HFS of the surrounding protons. The correlation time of the probe rotation in the liposome membranes was $\tau_c \gtrsim 10^{-7}$ s at 260 K within the Brownian diffusion model.

The changes caused by relaxation in the ESR spectra of probe IV in membranes are registered at the temperature above 200 K. The same changes in the ESR spectra of probe V reveal themselves at higher temperatures ($T \gtrsim 240$ K), however, they exhibit a sharper temperature-dependence. These differences can be explained by the assumption that a positively charged nitroxyl fragment of probe IV is accessible to water being located at the surface polar sites of the liposome membrane [32], whereas the N–O fragment of probe V is in its softer lipid part [33].

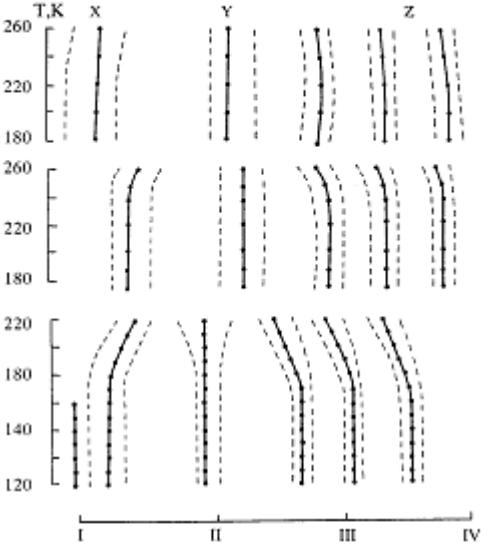

Fig.7. The plot of the position (solid curve) and half-width (dotted curve) of the ESR spectra components of radicals: a IV, b V in liposome membranes and c VI in ethanol vs. temperature [32]. I–IV – positions of the Mn^{2+} standard components.

The observed changes in the line shape are of a complicated character, therefore more than one parameter, e.g., the correlation time, is needed for their description. However, a qualitative conclusion can be made, namely, the frequency of probe mobility in the membranes at 260 K does not exceed 10^7 s^{-1}, and the dependence of mobility on the temperature is mainly determined by the environment closest to the probe. Thus, for probe IV, located in the surface layers of the membrane, the mobility increase at $T > 200$ K is probably caused by melting of the surface water matrix. An active fragment of probe V is in a more rigid lipid part of the membrane adjacent to the surface layers. At higher temperature the fragment conformation is changed and the increase of its mobility proceeds more sharply.

The comparison between the magnetic constants for the membranes modified by probe V and for model systems with the similar radicals leads to the conclusion that the structure and polarity of microenvironment are close for probe V in membranes and probe VII in the frozen methanol matrix.

Inverted Micelles. Solutions of surface active substances (SAS) in organic solvents are considered to be perspective systems for various biochemical processes [34]. Due to the polar core, the inverted micelles acquire the ability of solubilizing ions, polar substances and a large number of water molecules. The catalytic activity of the protein engaged into the inner space of the micelles depends strongly on the polarity of the inner space and the structure of the micelles shell [35]. The properties of the micelle-protein system were studied using spin labels and probes at the 3 cm wave band [6,35,36]. However, insufficient spectral resolution at this band did not allow to apply this method to the study of structural and dynamic parameters of this system.

The results of the 2 mm wave band ESR investigation of the microenvironment polarity and dynamic properties of paramagnetic probe VII in the system shell of inverted micelles of sodium diisooctylsulfosuccinate in octane, containing solubilized protein α-chymotrypsin [37] are given below. The samples were obtained according to [35].

The magnetic constants of paramagnetic probe VII in frozen micellar systems with the hydration degree ($R=[H_2O]/[SAS]$) from 0 to 80 and in some model systems are listed in the Appendix.

The comparison of corresponding magnetic constants of micellar and model systems shows that probe VII in the micelle shell practically has a nonpolar environment and its magnetic parameters depend weakly on the hydration degree, R. Consequently, the radical fragment is localized in the hydrophobic zone of the micelle shell and does not interact with the water molecules. Slight changes in the magnetic constants of the probe at the changes in the system composition can be explained by the effect of the hydration degree on the size and general state of the micelle shell. The obtained data do not confirm the conclusion made in [35], where anomalously low A_{zz} value of probe VII in the hydrated micelles are explained by its different localization in the matrix.

As the temperature increases above 200 K, the components of the ESR spectra of the probe VII in micellar systems are broadening and shifted due to the increase of molecular mobility (Fig.8). At 260 K the spectrum components are overlapped into a wide (2 mT) singlet corresponding to the radicals with the rotation frequency of $\nu_1 \approx 10^8$ s^{-1}. This singlet is practically overlapped by a triplet corresponding to the radicals with the rotation frequency of $\nu_2 \approx 10^{10}$ s^{-1} (see Fig.8). The change in the hydration degree from 3 to 80 leads to the increase in the g-factor of the second paramagnetic center. This shows that 4% of the probe molecules are beyond the lipid layer, their mobility is high and they interact with water molecules solubilized in the inner space of the micelles. The difference between the g-factors of both paramagnetic centers can be explained by the different conformation of the radical microenvironment in the shell and in the inner space

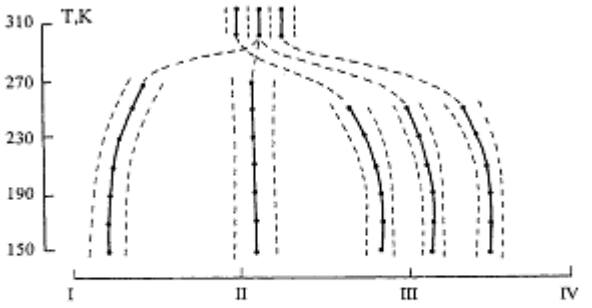

Fig.8. The plot of the position (solid curve) and half-width (dotted curve) of the uniform ESR spectrum components of radical VII in inverted micelles vs. temperature [37]. I–IV = the positions of the Mn standard components.

of the micelles, and by the dependence of the conformation of the radical microenvironment on the hydration degree.

The comparison of the experimental ESR spectra with those theoretically calculated by Antsiferova [37] showed that the addition of protein to the micellar system resulted in the two-fold decrease in the activation energy of the probe rotation. It shows the higher rigidity of the micelle structure at such transition. The reverse effect is observed at the increase in the hydration degree of micelles with protein.

The obtained data can be explained by the cooperative effect of water and bioglobule produced on the micelle structure, microenvironment and mobility of the probe being remote from the interface.

α-Chymotrypsin. The catalytic activity of α-chymotrypsin depends on the structural organization and molecular mobility in the vicinity of its active center [38]. The introduction of a spin label to the zone of enzymatic reaction gives valuable information on the structural and dynamic parameters of this site which can be compared with the catalytic activity of α-chymotrypsin.

The results of the study of structural and dynamic characteristics of the environment of spin label I bound to methionin-192 group [39] in the region of the α-chymotrypsin active centers are presented in this section. The study of the enzyme of 0.04–0.96 humidity were carried out in the temperature range 150–320 K.

The ESR spectra of lyophilized spin-labelled α-chymotrypsin at 150 K are characterized by lower inhomogeneous broadening of the canonic components as compared with the egg lysozyme, which can be explained with higher homogeneity of the label environment in α-chymotrypsin. Neverthe-

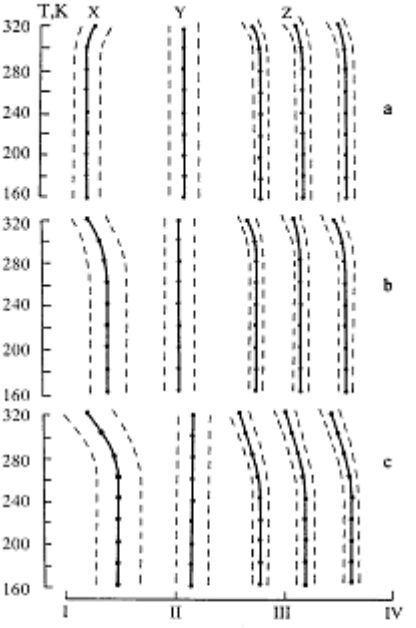

Fig.9. The plot of the position (solid curve) and half-width (dotted curve) of the ESR spectra components of radical I in α-chymotrypsin with the 0.04 (**a**), 0.65 (**b**) and 0.96 (**c**) value of relative humidity degree vs. temperature. I–IV – positions of the Mn^{2+} standard components.

less a considerable broadening of the spectra components of the sample of 0.96 humidity (Fig.9) is observed which can be caused by the conformational changes in the sample during its wetting.

The magnetic parameters g_{xx} and A_{zz} of radical I located in the vicinity of the active center of frozen α-chymotrypsin relative humidity of 0.04, 0.65 and 0.96 are presented in Fig.5. As seen from Fig.5, the magnetic parameters of lyophilized sample practically coincide with the general correlation between g_{xx} and A_{zz} of model systems. This demonstrates the similarity of the polarity and structure of radical I environment in the lyophilized sample and ethanol matrix. For the sample saturated by water the active fragment of label I (like in the case of HSA) is solvated with its molecules forming n=o

radical complex. It is seen from the gradual changes in its magnetic parameters. The polarity of the radical microenvironment increases by 1.4 and 1.8 times for the increase of the relative humidity from 0.04 to 0.65 and 0.96, respectively. Different slopes of the correlation plots (g_{xx} and A_{zz}) of radical I in model systems and α-chymotrypsin may probably indicate the predominance of the donor-acceptor radical complex over the electrostatic one in this biological system.

The ESR spectra of the lyophilized spin-labelled α-chymotrypsin did not exhibit any changes caused by relaxation in the line shape up to 290 K which is explained by the rigid fixing of the radical fragment by the groups surrounding it. At higher temperature the label mobility increases (see Fig.9a). The correlation times of the label rotation defined from the ESR spectra were equal to $\tau_c = 6 \cdot 10^{-19} \exp(-8.0 \cdot 10^4 / \mathscr{R} T)$ and the efficient microviscosity in the place of the radical location at 300 K was 72 Pa s.

At damping of the sample the molecular mobility is registered at lower temperature (Figs.9b and 9c). The analysis of the experimental data showed that the rotation of the radical I in α-chymotrypsin proceeds around the *y*-axis with the correlation time of $\tau_c = 3.6 \cdot 10^{-12} \exp(-2.6 \cdot 10^4 / \mathscr{R} T)$ and $\tau_c = 4.1 \cdot 10^{-11} \exp(-1.8 \cdot 10^4 / \mathscr{R} T)$ at humidity of the sample of 0.65 and 0.96, respectively. The value of the efficient viscosity in the place of the radical location decreased from 72 to 14 and 7 Pa s with the increase in the relative humidity from 0.04 to 0.65 and 0.96. In contrast to the lyophilized sample, the *x*-component of the ESR spectra of damped α-chymotrypsin samples shifts to weaker fields at heating (Figs.9b and 9c). This effect and the same effects in other spin-labelled biological systems may be explained by the weakening of the hydrogen bond of the radical complex in the damped α-chymotrypsin as temperature increases which is defined by the value of the relative humidity.

Thus, the molecular motion of label I in lyophilized α-chymotrypsin is hindered by the strong interaction of its nitroxyl fragment with hydroxyl groups. In the radical complex the latter are partially substituted by water molecules during the sample damping which leads to the increase in the radical dynamics. Since the motion of the label in egg lysozyme of relative humidity up to 0.8 was completely frozen, the conclusion can be made that the radical in α-chymotrypsin has some odd degrees of freedom as compared to lysozyme and is located in the hydrophobic pocket of other structure. This is confirmed by the difference in the axis of the predominant radical rotation and the character of its interaction with the environment in these systems. The correlation time of radical rotation in α-chymotrypsin decreases down to $5.5 \cdot 10^{-12}$ s in the above mentioned micellar systems with the hydration degree, $R = 6$ [35].

Cotton Fibre and Cellulose. To determine the mechanisms of chemical conversions in the cotton fiber and cellulose it is necessary to know their microstructure and dynamic properties. The ESR spectroscopy is widely applied

to the solution of this problem [40,41]. However, in the case of these natural biopolymers as well as in the above discussed ones, low spectral resolution of the conventional 3 cm ESR wave band does not give the complete picture of the processes in these systems.

The ESR method of high spectral resolution was used in the study of structural and dynamic parameters of the modified cotton fiber [42] and microcrystalline cellulose [43].

The cotton fiber from the 5595-V and Tashkent-1 cotton strains and microcrystalline cellulose (C) amorphised under the $2 \cdot 10^9$ Pa pressure between the Bridgman anvils with 10° and 400° shift (CA−I and CA−II, respectively) were investigated. The spin labelled by radical VIII cotton fiber and cellulose modification was carried out according to [44]. The C and CA−I samples were exhibited to ^{60}Co-radiation (10 MRad, 290 K) in the air.

At 150 K the ESR spectra of the lyophilized spin-labelled systems as those of egg lysozyme are characterized by the considerable broadening of the canonical lines caused by the interaction of the nitroxyl fragment with the hydroxyl groups of proteins. The magnetic constants of radical VIII in the biological and model systems estimated from their ESR spectra are given in Appendix.

The values of magnetic constants g_{xx} and A_{zz} of radical VIII are summarized in Fig.10. Figure shows that the magnetic parameters of 5595-V and Tashkent-1 samples correspond to the obtained correlation between g_{xx} and A_{zz} for the model systems. It leads to the conclusion that the structure and the polarity of the microenvironment of the radical VIII are identical in the Tashkent-1 sample and ethanol matrix as well as in the 5595-V sample and water matrix.

Quite a different picture is observed for the spin-labelled sample of cellulose and cotton fibre from Vylt-infected Tashkent-1. Their magnetic constants do not follow the general correlation between g_{xx} and A_{zz} of frozen model systems (see Fig.10). It can be explained by conformational difference in the label VIII microenvironment in these biological polymers.

At heating of the 5595-V and C samples the x-components of their ESR spectra gradually shift into the weak fields (Figs.11a and 11b, respectively). As in the case of lysozyme, most probably it is caused by the weakening of the hydrogen bond between the radical fragment and molecules of the microenvironment at elevated temperatures.

At 315 K the y-component of the ESR spectrum of the lyophilized sample of 5595-V is a superposition of at least two lines, i.e. a wide singlet and a triplet with $g = 2.00610$ and $a = 1.52$ mT (Fig.11a). The triplet is due to the presence of the amorphous regions of high radical mobility ($\tau_c \leq 2.2 \cdot 10^{-10}$ s, 335 K). The estimate of the radical portion in the amorphous phase (about 2%) is in agreement with the value obtained earlier at 3 cm wave band [40].

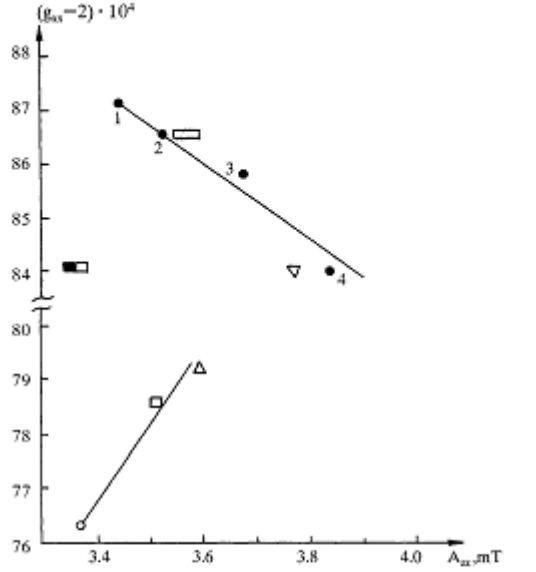

Fig.10. The correlation plot (g_{xx} and A_{xx}) for radical VIII in frozen (150 K) octane (1), ethanol (2), methanol (3), water-glycerol (10:1) mixture (4) and in cotton fibres "Tashkent-1" (open rectangle), "Tashkent-1" infected by Vylt (semipainted rectangle), 5595-V (triangle down), cellulose samples C (circle), CA–I (triangle up) and CA–II (square) with the value of relative humidity degree of 0.04 [42,43].

The difference in the label isotropic *g*-factors in the crystalline (2.00553) and amorphous (2.00610) phases is in agreement with the shift of the *x*-component to the weak fields as the temperature increases. It shows that the intensification of the molecular motion in the amorphous regions of the 5595-V sample is accompanied by the weakening of the radical hydrogen bond with the microenvironment.

The existence of different phases in cellulose was not registered.

The heating of the spin-labelled 5595-V sample results in the shift (0.7 mT) and the broadening (0.08 mT) of the *z*-component (Fig.8). This weak broadening of the line along with a considerable shift disagrees with the model of Brownian isotropic rotation and with the model of large angle

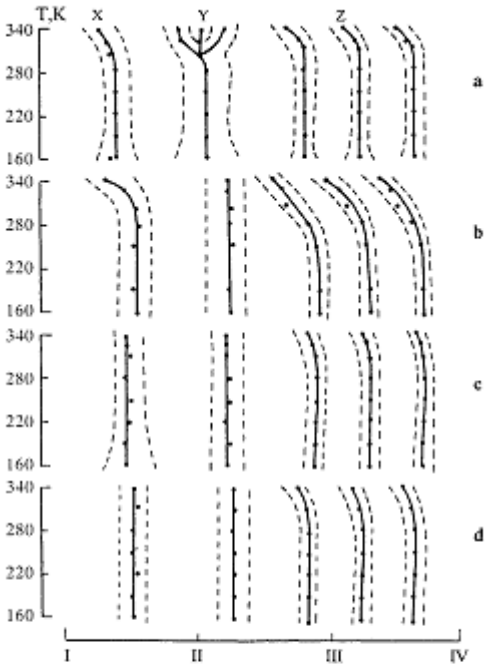

Fig.11. The plot of the position (solid curve) and half-width (dotted curve) of the ESR spectra components of radical VIII in lyophilized cotton fibres 5595-V (a), cellulose samples C (b), CA–I (c) and CA–II (d) vs. temperature [42,43]. I–IV – positions of the Mn^{2+} standard components.

jumps [40,45]. This effect can be explained either by the compensative narrowing of the line due to the decrease in the inhomogeneous broadening or by the presence of fast torsion oscillations of the radical fragment near the *x*-axis [46] with the frequency of $10^9\ s^{-1}$ and amplitude of $10\pm3^\circ$ (335 K).

The analysis of the temperature dependence of broadening and the shift of the *z*-component of the ESR spectra of the spin-labelled cellulose samples (Figs.11b–11d) as well as the comparison with the corresponding changes in theoretically calculated ESR spectra [47] leads to the conclusion about the

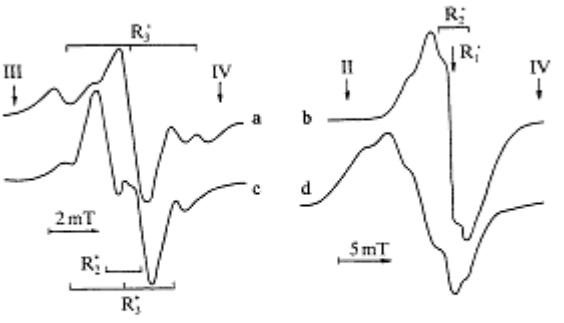

Fig.12. The ESR spectra of γ-radiated (10 MRad) samples of lyophilized cellulose C (a,b) and CA−II (c,d) registered at 290 K in 3 cm (a,c) and 2 mm (b,d) wave bands [43]. II−IV − positions of the Mn^{2+} standard components.

Brownian rotation of label VIII around the axis of the preferable rotation in the *xz*-plane of the molecular coordinate system.

The amorphization of the sample C leads to the damping of the label mobility in CA−I and to partial reduction of the elasticity of the label environment (see Fig.11b). The correlation time, τ_c, of the radical VIII rotation in C, CA−I and CA−II samples calculated from the ESR spectra are equal to $2.3 \cdot 10^{-4}\exp(-1.9 \cdot 10^4/\mathscr{R}T)$, $36 \cdot \exp(-4.6 \cdot 10^4/\mathscr{R}T)$ and $5.0 \cdot 10^{-2} \times \exp(-3.1 \cdot 10^4/\mathscr{R}T)$ s, respectively.

Thus, the radical mobility is mainly determined by the shape of the cage which radical occupies in cellulose, and the degree of its treatment which is likely to decrease the space size and to effect the system conformation. The treatment effect reflects probably the change in conformation of the macromolecule and its monomeric subunits.

To confirm the latter supposition the ESR spectra of γ-radiated C (a, b) and CA−II (c, d) samples were registered at the 3 cm (a, c) and 2 mm (b, d) wave bands at 290 K (see Fig.12).

The comparison of the ESR spectra enables to make a conclusion that in C sample there are at least three paramagnetic centers of different magnetic constants (see Fig.12): R_1' is a singlet ($g_1 = 2.00281$), R_2' is a doublet ($g_2 = 2.00295$ and $a_2 = 2.9$ mT) and R_3' is a triplet ($g_3 = 2.00442$ and $a_3 = 2.7$ mT). This observation is mainly in accordance with the results of the computer simulation of the 3 cm ESR spectra of the γ-radiated C sample [41]. The R_1' line can be attributed to contamination by lignin [41].

The formation of $R_2^{\bullet}$ and $R_3^{\bullet}$ centers can be explained by the process of dehydrogenation of the glucopyranose cycle in the C_1 and C_4 positions, respectively.

In CA–II after its radiation at least two additional paramagnetic centers appear (see Fig.12): $R_2^{\bullet}$ is a doublet ($g_2^{\bullet}$=2.00505 and $a_2^{\bullet}$=1.5 mT) and $R_3^{\bullet}$ is a triplet ($g_3^{\bullet}$=2.00532 and $a_3^{\bullet}$=2.2 mT). Since the C monomer unit can exist in different conformation the formation of these centers in CA–II can be explained by dehydrogenation of a glucopyranose cycle (conformation of which is different from the initial one) in the C_1 and C_4 positions, respectively.

5. Anisotropic Slow Molecular Rotations Studied by the Method of RF Saturation Transfer at the 2 mm Wave Band ESR

As is known, the "linear" ESR method is used to study the molecular processes in biological and other systems with the correlation time of $\tau_c = 10^{-11}$–10^{-7} s. However the slow transformations with characteristic time of $\tau_c \geq 10^{-7}$ s are realized in major biological native systems. These processes can be studied with the help of the RF saturation transfer ESR (ST ESR) method [5,48].

According to the ST ESR approach, the shape of ESR spectrum of the spin-labelled system registered at saturation:

$$\gamma^2 H_1^2 T_1 T_2 \gg 1 \tag{6}$$

and at adiabatic fast passage of a resonance:

$$\mathrm{d}H/\mathrm{d}t = \gamma H_m \omega_m \ll \gamma^2 H_1^2 \tag{7}$$

(γ is the gyromagnetic ratio, H_1 is the magnetic component of the MW field in the sample, T_1 and T_2 are the spin-lattice and spin-spin relaxation times, respectively, $\mathrm{d}H/\mathrm{d}t$ is the rate of the magnetic field change, H_m and ω_m are the amplitude and angle frequency of the ac modulation field, respectively) is sensitive both to their effective relaxation time and slow ($10^{-7} \leq \tau_c \leq 10^{-3}$ s) molecular motions. In-phase and $\pi/2$ out-of-phase components of the dispersion and absorption signals are more sensitive to such coincident relaxation and dynamic processes [5,24].

As a rule, the motion in biological systems is an anisotropic one. For example, a radical can easily rotate only around x-axis. Consequently, conditions of Eq.(6) and Eq.(7) may not be valid at slow molecular motions in

which radicals whose y- and z-axes are oriented along the external magnetic field participate. In this case the spectral diffusion of RF saturation is realized and the amplitude of the y- and z-spectral components is decreased. The theoretical analysis shows that at low frequency of registration the determination of the preferable radical rotating axis as well as the separate registration of the radical relaxation and motions are impossible because of overlapping of the ST ESR principal components [5].

These limitations are partly eliminated in the case of the registration of ST ESR spectra at higher frequency. However, the anisotropy of the g-factor and HFI at frequencies up to 30 GHz is comparable [49], so the overlapping of the ST ESR spectral components remains.

Earlier [50,51] we have shown that above mentioned limitations of the ST ESR method may be eliminated completely by recording of ESR spectra at 2 mm wave band. According to theory, the rate of MW saturating transfer at the spectrum as well as the spectrum shape's sensitivity to low anisotropic molecular motion should increase.

The ESR and ST ESR spectra of the radical IX and X solutions in tertbutylbenzene (10^{-2} M) were registered at 90–300 K and H_1=20 μT. These radicals are characterized by highly anisotropic rotation in the model systems around the x- and y-axes, respectively. The magnetic constants of radicals IX and X are listed in Appendix.

At $T \geq 180$ K the motion of the radicals is anisotropic with the correlation time of $\tau_c \leq 10^{-7}$ s. The extrapolation to the 160 K gave the value of $\tau_c = 5 \cdot 10^{-7}$ s. At $T < 170$ K the shape of the first harmonic of the in-phase absorption does not practically change. Marked changes in the bell-like ST ESR spectra are observed in the range of 130–170 K.

Theoretical calculations made by Livshits [51] showed that the ratio of the amplitude of the second harmonic of $\pi/2$ out-of-phase to that in-phase components of the absorption signal is sensitive only to the time of spin-lattice relaxation, T_1. The ratio of the amplitude of the components of its $\pi/2$ out-of-phase ST ESR spectra is sensitive to the radical rotation.

For example, the amplitude ratio of the x- and y-components of the $\pi/2$ out-of-phase ST ESR spectra of radical IX increases from 0.4 to 0.75 at 130–170 K (Fig.13a), which evidences for the increase in its rotation rate around the x-axis with the correlation time of $\tau_c \geq 4 \cdot 10^{-6}$ s, whereas the value of the spin-lattice relaxation time T_1 changes by 6–10 times.

More considerable changes are registered for radical X (Fig.13b). The same temperature increase leads to the decrease in the correlation time of this radical rotation by more than two orders of magnitude (10^{-5}–10^{-7} s) at the very slight (1.5–2 times) decrease in the T_1 value.

Thus, the changes in the ST ESR spectra of radical IX are caused both by the decrease in the value of spin-lattice relaxation time T_1 and radical rota-

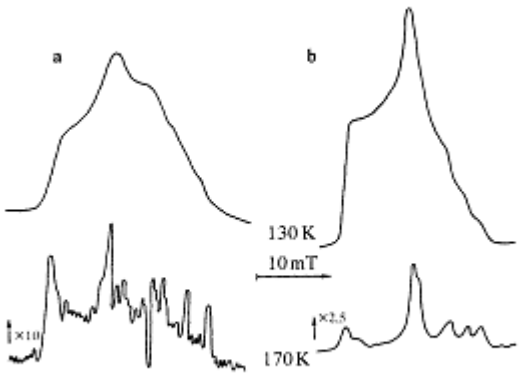

Fig.13. The second harmonic $\pi/2$ out-of-phase of absorption signals of radical IX (a) and X (b) solutions in terthutylbenzene at 130 and 170 K [50,51].

tion around the x-axis, those of radical X – mainly by intensification of very slow rotation around its long axis. If spin-lattice relaxation is mainly determined by very fast molecular motions limited in their amplitude, the rotational mobility is characterized by slower ($\tau_c \approx 10^{-5}$–10^{-7} s) motion with relatively large angular amplitude. The differences in the dynamics of IX and X radicals perhaps can be explained by their structure difference and the peculiarities of interaction with the environment.

Consequently, the 2 mm ST ESR registration essentially expands the potential of the method in the investigation of anisotropic very slow molecular mobility in various biological systems.

6. Identification of the Paramagnetic Centers via the 2 mm Band ESR Spectra

ESR spectroscopy is widely used for the study of metabolic and radiation-induced reactions in biological systems, in which the paramagnetic centers are formed as a transient and final product [52]. The analysis of nature and character of these centers gives the possibility to study the reactions and structural, conformational and dynamic properties of radical microenvironment in the biological systems.

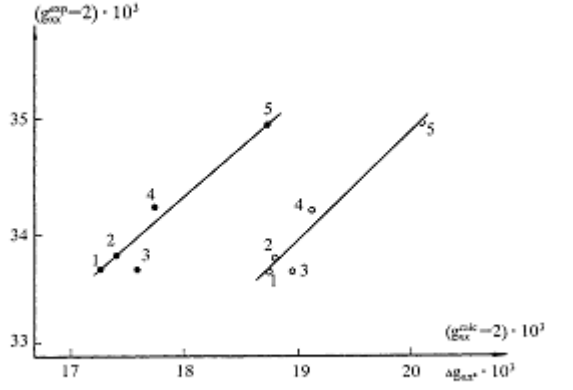

Fig.14. The correlation plots (g_{xx}^{exp} and g_{xx}^{calc}) and (g_{xx}^{exp} and Δg_{xx}^{calc}) peroxyradicals $C_3H_7CH_2OO$ (1), $C_3H_7(CH_3)_2COO$ (2), $(CH_3)_3COO$ (3), $C_2H_5(CH_3)_2COO$ (4) and $C_2H_5CH_2OO$ (5) [57].

The paramagnetic centers with unpaired electrons localized on the carbon or sulfur atoms are as a rule primary radicals in biological systems. In the first case, the g-factor of the paramagnetic center is usually close to that of the free electron (g_e=2.00232). HFI of the unpaired electron with the other nuclei of the nonzero nuclear spin is easily analyzed according to the ESR spectra in the wide range of registration frequency [52–54]. The localization of the unpaired electron on the sulfur atom causes a substantial deviation of the g-factor from the g_e and leads to its tensor character. Magnetic parameters of such a center are also determined from the ESR spectra in the usually used 3 cm wave band [55].

Peroxide radicals (PR) are rather formed as intermediate and final products in biological systems. The unpaired electron in such centers localizes mainly on the O–O fragment, therefore HFS is absent, the values of their g-factors are close to each other [55], and the identification of PR in the 3 cm ESR spectra is difficult.

As in the case of registration of nitroxide radicals at the 2 mm wave band of ESR, all the components of the PR's ESR spectra are resolved [56]. Simultaneous registration of paramagnetic centers which are different in their nature but close in their g-factors is possible at this band. In [57] the possibility of identification of the organic PR via their paramagnetic constants (see Appendix) was analyzed.

In the case of PR the main contribution to the *g*-factor is made by the $n-\pi^*$ excited electron configuration [58]. To check the possibility of PR identification, the comparison of the experimental magnetic parameters of some PR and those theoretically calculated by Dmitruk [57] was undertaken.

The correlation of experimental and theoretical magnetic parameters of some primary and tertiary PR are represented in Fig.14. The Δg_{zz}^{calc}-shift of the *g*-factor is caused by the $n-\pi^*$ transition. For secondary PR the calculation gives anomalously low values of magnetic constants [57].

As seen from Fig.14, the magnetic parameters of organic PR are strongly dependent on the donor-acceptor and conformational properties of their substituents. It gives the possibility of identification of the primary and tertiary PR formed in biological systems.

Thus, the ESR spectroscopy of high resolution allows the identification of the paramagnetic centers of different nature with close *g*-factors and the use of stable (for example, $(C_6H_5)_3COO$) PR as spin labels in the study of biological macromolecules.

7. Conclusion

The present mini-review shows that the 2 mm wave band ESR spectra permit to obtain qualitatively new information in such fields as metrology of free radicals, spin labels and probes, molecular mobility, electron and spatial structures of paramagnetic centers, local environment effects, etc. Separate registration of the ESR spectra of paramagnetic centers of different nature makes possible the analysis of structural and dynamic characteristics of spin-labelled biological objects.

Thus, the ESR spectroscopy of high resolution combined with the method of spin labels and probes gives a unique possibility of analyzing the structure and dynamic transitions in various biological systems. The above results show the high resolution ESR spectroscopy to be an efficient method for the solution of a wide range of problem in chemical and biological physics.

The further development of the method seems to lie in its combination with pulsed methods and Fourier data processing.

Acknowledgements

The author expresses his sincere gratitude to Prof. G.I.Likhtenstein and Dr. A.V.Kulikov for their permanent attention to this work and valuable criticism, to Prof. Ya.S.Lebedev and Dr. O.Ya.Grinberg for their participation in the discussion of the results.

Appendix

1. Magnetic constants of nitroxyl radicals in frozen biological and model systems [17].

Matrix	R	g_{xx}	g_{yy}	g_{zz}	g_{av}	A_{zz}(mT)
		Radical I				
Toluene	–	2.00953	2.00577	2.00176	2.00569	3.40
n-Butanol	–	2.01010				
		2.00935	2.00602	2.00197	2.00578	3.50
Ethanol	–	2.00910	2.00573	2.00210	2.00564	3.58
Ethanol+water	0.25	2.00902	2.00543	2.00212	2.00552	3.60
Ethanol+water	0.50	2.00890	2.00602	2.00214	2.00569	3.65
Ethanol+water	0.66	2.00883	2.00608	2.00201	2.00564	3.70
Methanol	–	2.00860	2.00550	2.00178	2.00529	3.73
Water+glicerol	0.90	2.00834	2.00571	2.00167	2.00524	3.77
HSA	0.04	2.00893	2.00585	2.00164	2.00547	3.60
HSA	0.96	2.00842	2.00570	2.00170	2.00527	3.75
Lysozyme	0.04	2.00946	2.00646	2.00217	2.00603	3.50
Lysozyme	0.35	2.00923	2.00617	2.00220	2.00587	3.61
Lysozyme	0.60	2.00912	2.00614	2.00214	2.00580	3.69
Lysozyme	0.80	2.00908	2.00603	2.00211	2.00574	3.74
Lysozyme	0.96	2.00902	2.00624	2.00211	2.00579	3.85
α-chymotrypsin	0.04	2.00912	2.00598	2.00210	2.00573	3.58
α-chymotrypsin	0.65	2.00859	2.00613	2.00219	2.00564	3.67
α-chymotrypsin	0.96	2.00828	2.00583	2.00209	2.00540	3.73
		Radical II				
HSA	0.04	2.00998				
		2.00883	2.00612	2.00216	2.00570	3.64
HSA	0.96	2.00863	2.00613	2.00215	2.00563	3.84
		Radical III				
HSA	0.04	2.00855	2.00621	2.00214	2.00563	3.55
HSA	0.96	2.00845	2.00614	2.00210	2.00556	3.67
		Radical IV				
Membranes	–	2.00980	2.00642	2.00232	2.00618	3.67
		Radical V				
Membranes	–	2.00918	2.00614	2.00230	2.00587	3.60
		Radical VI				
Ethanol	–	2.01044				
		2.00984	2.00696	2.00302	2.00661	3.39
		Radical VII				
Octane	–	2.00951	2.00611	2.00215	2.00592	3.28
n-Propanol	–	2.00955				
		2.00894	2.00619	2.00217	2.00597	3.29
Ethanol	–	2.00901	2.00617	2.00219	2.00597	3.42
Methanol	–	2.00882	2.00626	2.00228	2.00579	3.61
Micelles without	0	2.00952	2.00626	2.00226	2.00601	3.41
the protein	3	2.00946	2.00614	2.00213	2.00591	3.32
Micelles with	3	2.00954	2.00622	2.00221	2.00599	3.34
the protein	6	2.00958	2.00622	2.00231	2.00603	3.41
α-chymotrypsin	10	2.00950	2.00618	2.00215	2.00594	3.36
α-chymotrypsin	15	2.00954	2.00622	2.00220	2.00599	3.41

Matrix	R	g_{xx}	g_{yy}	g_{zz}	g_{iso}	A_{zz}(mT)
α-chymotrypsin	20	2.00950	2.00622	2.00230	2.00601	3.36
α-chymotrypsin	30	2.00946	2.00621	2.00222	2.00597	3.41
α-chymotrypsin	40	2.00939	2.00618	2.00217	2.00591	3.32
α-chymotrypsin	50	2.00943	2.00614	2.00217	2.00591	3.32
α-chymotrypsin	60	2.00946	2.00622	2.00226	2.00598	3.35
α-chymotrypsin	80	2.00937	2.00607	2.00210	2.00585	3.34
		Radical VIII				
Octane	–	2.00872	2.00633	2.00214	2.00573	3.43
Ethanol	–	2.00865	2.00622	2.00221	2.00569	3.52
Methanol	–	2.00857	2.00617	2.00209	2.00560	3.69
Water+glycerol	0.90	2.00840	2.00627	2.00215	2.00561	3.81
Cotton 5595-V	0.04	2.00842	2.00592	2.00224	2.00553	3.76
Cotton "Tash-1"	0.04	2.00863	2.00622	2.00232	2.00572	3.55
Cotton + Vylt	0.04	2.00840	2.00562	2.00212	2.00538	3.35
C	0.04	2.00762	2.00582	2.00211	2.00518	3.37
CA–I	0.04	2.00791	2.00584	2.00222	2.00532	3.57
CA–II	0.04	2.00783	2.00574	2.00227	2.00528	3.49
		Radical IX				
Tertbutylbenzene	–	2.00979	2.00622	2.00206	2.00602	3.41
		Radical X				
Tertbutylbenzene	–	2.00947	2.00541	2.00217	2.00568	3.12

Note: The measurement errors in the component of g- and A-tensors are $7 \cdot 10^{-5}$ and $3 \cdot 10^{-2}$ mT, respectively. R is the relative H_2O content (in model systems), hydration degree (in micelles) and the value of relative humidity (in other biosystems).

2. Magnetic constants of organic peroxyradicals in model systems [56].

Radical	Matrix	g_{xx}	g_{yy}	g_{zz}	g_{iso}
HOO	$H_2O_2+H_2O$	2.0329	2.00806	2.00331	2.01478
$(CF_3(CF_2)_6)_2CFOO$	self	2.0381	2.00742	2.00231	2.01596
$CF_3(CF_2)_6CF_2OO$	self	2.0396	2.00770	2.00277	2.01670
$C_6H_{11}OO$	self	2.0340			
		2.0306	2.00815	2.00279	2.01498
$(C_6H_5)_2COO$	$(C_6H_5)_2CCl$	2.0310	2.01445	2.00200	2.01581
$(C_6H_5)_2CHOO$	self	2.0346	2.00792	2.00212	2.01488
$Br(C_6H_4)C(CH_3)_2OO$	self	2.0328			
		2.0228	2.00792	2.00236	2.01436
$(C_6H_5)C(CH_3)_2OO$	self	2.0334			
		2.0302	2.00824	2.00253	2.01472
$(CH_3)_3COO$	self	2.0336	2.00830	2.00237	2.01476
$C_2H_5(CH_3)_2COO$	self	2.0342	2.00859	2.00267	2.01415
$C_3H_7(CH_3)_2COO$	self	2.0337	2.00801	2.00251	2.01474
$C_3H_7(CH_3)HCOO$	self	2.0340			
		2.0295	2.00823	2.00240	2.01487
$C_3H_7CH_2OO$	self	2.0336	2.00816	2.00358	2.01511
$C_2H_5CH_2OO$	^{t}Bu-butyrate	2.0349	2.00792	2.00271	2.01518
$CH_3CONHCHC_3H_7$ (OO)	self	2.0323	2.00802	2.00187	2.01418

Radical	Matrix	g_{xx}	g_{yy}	g_{zz}	g_{iso}
$CH_3CON(CH_3)CH_2OO$	self	2.0350	2.00792	2.00180	2.01490
$CH_3CON(C_2H_5)C_2H_4OO$	self	2.0351			
		2.0309	2.00780	2.00181	2.01489
$CH_3CONHCHCH_2$ | OO	self	2.0320	2.00766	2.00339	2.01435

Note: The measurement errors of the g_{xx} and g_{yy}, g_{zz} values are $2 \cdot 10^{-4}$ and $3 \cdot 10^{-5}$, respectively. The magnetic constants of alkyl radicals formed in some systems are not listed. Peroxy-radicals were produced mainly by photolysis of respective hydroperoxyd at 77 K.

References

[1] Konev, S.V.: Electron Excited States of Biopolymer (Russ), Minsk: Nauka i Tekhnika 1965.
[2] Goldansky, V.I.: Mosshauer Effect and Its Application to Chemistry (Russ), Moskou: USSR Acad.Nauk Publ. 1963.
[3] Kiselyov, N.A.: Electron Microscopy of Biological Molecules (Russ), Moskou: Nauka 1965.
[4] Berliner, L. (ed.): Spin Labeling. Theory and Application. 1, New York: Academic Press 1976.
[5] Berliner, L. (ed.): Spin Labeling. Theory and Application, 2, New York: Academic Press 1979.
[6] Likhtenstein, G.I.: Spin Labels in Molecular Biology (Russ), Moskou: Nauka 1974.
[7] Likhtenstein, G.I.: Chemical Physics of Metalloenzyme Catalysis, Heidelberg: Springer Verlag 1988.
[8] Dudich, I.V., Timofeev, V.P., Volkenstein, M.V., Misharin, A.Ju.: Molecul.Biologiya. 11, 685–689 (1977)
[9] Isaev-Ivanov, V.V., Lavrov, V.V., Fomichev, V.N.: Dokl.Akad.Nauk SSSR. 229, 70–72 (1976)
[10] Hyde, J.S., Dalton, L.: Chem.Phys.Lett. 16, 568–572 (1972)
[11] Hwang, J.S., Mason, R., Hwang, L.P., Freed, J.H.: J.Chem.Phys. 79, 489–511 (1975)
[12] Grinberg, O.Ya., Dubinsky, A.A., Shuvalov, V.F., Oransky, L.G., Kurochkin, V.I., Lebedev, Ya.S.: Dokl.Akad.Nauk SSSR. 230, 884–886 (1976)
[13] Ondar, M.A., Grinberg, O.Ya., Dubinsky, A.A., Lebedev, Ya.S.: Khimich.Fizika (Russ) 3, 527–536 (1984)
[14] Grinberg, O.Ya., Dubinsky, A.A., Poluektov, O.G., Lebedev, Ya.S.: Khimich.Fizika (Russ) 6, 1363–1372 (1987)
[15] Dubinsky, A.A., Grinberg, O.Ya., Kurochkin, V.I., Oransky, L.G., Poluektov, O.G., Lebedev, Ya.S.: Teoretich. i Eksperim. Khimiya. 17, 231–237 (1981)
[16] Lynch, W.B., Earle, K.A., Freed, J.H.: Rev.Sci.Instrum. 59, 1345–1351 (1988)
[17] Krinichnyi, V.I.: Zurn.Prikl.Spektr. 52, 887–905 (1990)
[18] Buchachenko, A.L., Wasserman, A.M.: Stable Radicals (Russ), Moskou: Khimiya 1973.
[19] Buchachenko, A.L.: Complexes of Radicals and Molecular Oxygen with Organic Molecules (Russ), Moskou: Nauka 1984.
[20] Reddoch, A., Konishi, S.: J.Chem.Phys. 70, 2121–2128 (1979)
[21] Kivelson, D.: J.Chem.Phys. 33, 1094–1111 (1960)
[22] McConnel, H.M.: J.Chem.Phys. 25, 709–711 (1956)
[23] Freed, J.H., Frankel, G.K.: J.Chem.Phys. 39, 326–348 (1963)
[24] Johnson, M.E., Lie, L.: Biochemistry, 21, 4459–4463 (1982)
[25] Galkin, A.A., Grinberg, O.Ya., Dubinsky, A.A., Kabdin, N.L., Krymov, V.N., Kurochkin, V.I., Lebedev, Ya.S., Oransky, L.G., Shuvalov, V.F.: Prib.Tekhnika Experim. 4, 284 (1977)
[26] Kuska, H.A., Rogers M.I. in: Radical Ions (Kaiser, E.T., Kevan, L. eds.) New York, London, Sydney: Interscl.Publ. 1968.

[27] Likhtenstein, G.I., Achmedov, Ju.D., Ivanov, L.V.: Molecul.Biologiya. 8, 48–52 (1974)
[28] Krinichnyi, V.I., Grinberg, O.Ya., Judanova, E.I., Lyubashevskaya, E.V., Antsiferova, L.I., Likhtenstein, G.I., Lebedev, Ya.S.: Biofizika 32, 215–220 (1987)
[29] Schmidt, P.O., Kuntz, I.D.: Biochemistry 23, 4261–4265 (1984)
[30] Krinichnyi, V.I., Grinberg, O.Ya., Bogatyrenko, V.R., Lebedev, Ya.S., Likhtenstein, G.I.: Biofizika 30, 216–219 (1985)
[31] Likhtenstein, G.I.: Polynuclear Redox Enzymes. Moskou: Nauka 1979.
[32] Krinichnyi, V.I., Grinberg, O.Ya., Yudanova, E.I., Boria, M.L., Lebedev, Ya.S., Likhtenstein, G.I.: Biofizika 32, 59–63 (1987)
[33] Griffith, O., Jost, P. in: Spin Labeling. Theory and Application (Berliner, L. ed.) 1, New York: Academic Press 1976.
[34] Fendler, J.H., Fendler, E.J.: Catalysis in Micellar and Macromolecular Systems, New York: Academic Press 1975.
[35] Belonogova, O.V., Likhtenstein, G.I., Levashov, A.V., Khmelnitsky, Yu.L., Klyachko, N.L., Martinek, K.: Biokhimiya 48, 379–386 (1983)
[36] Menger, F.M., Saito, G., Sanzero, G.V., Dodd, J.R.: J.Amer.Chem.Soc. 97, 909–911 (1975)
[37] Krinichnyi, V.I., Antsiferova, L.I., Lyubashevskaya, E.V., Belonogova, O.V., Grinberg, O.Ya., Likhtenstein, G.I.: Zura.Fizich.Khimii 63, 3015–3021 (1989)
[38] Levashov, A.V., Klyachko, N.L., Martinek, K.: Bioorganich Khimiya 5, 670–676 (1981)
[39] Kosman, D.J.: J.Molec.Biol. 67, 247–264 (1972)
[40] Yusupov, I.Kh., Bobodzanov, P.Kh., Marupov, R., Islomov, G., Antsiferova, L.I., Koltover, V.K., Likhtenstein, G.I.: Vysokomolekul.Soedin.(A) 26, 369–373 (1984)
[41] Yershov, B.G., Klimentov, A.S.: Uspekhi Khimii 53, 2056–2059 (1984)
[42] Krinichnyi, V.I., Grinberg, O.Ya., Yusupov, I.Kh., Marupov, R., Bobodzanov, P.Kh., Likhtenstein, G.I., Lebedev, Ya.S.: Biofizika 31, 482–485 (1986)
[43] Krinichnyi, V.I., Kostina, N.V.: Intern.Confer.Nitroxyl Radicals (Abstr.) Novosibirsk, 63, 1989.
[44] Marupov, R., Bobodzanov, P.Kh., Yusupov, I.Kh., Mavlyanov, A.M., Frolov, E.N., Likhtenstein, G.I.: Biofizika 24, 519–523 (1979)
[45] Poluectov, O.G., Lyubashevskaya, E.V., Dubinsky, A.A., Antsiferova, L.I., Lebedev, Ya.S.: Khimich.Fizika (Russ) 4, 1615–1618 (1985)
[46] Johnson, M.E.: Biochemistry 17, 1223–1228 (1978)
[47] Antsiferova, L.I., Lyubashevskaya, E.V.: The 2 mm Wave Band Spectra Atlas of the Nitroxyl Radicals, Chernogolovka: Izdat.Akad.Nauk SSSR 1986.
[48] Hemminga, M.A.: Chem.Phys.Lipids. 32, 323–383 (1973)
[49] Robinson, B.H., Dalton, L.R.: J.Chem.Phys. 72, 1312–1323 (1980)
[50] Lebedev, Ya.S., Antsiferova, L.I., Grinberg, O.Ya., Dubinsky, A.A., Krinichnyi, V.I., Lyubashevskaya, E.V., Poluektov, O.G.: 2-nd Conf.Modern Meth. RFS. DDR–8804, 48–57 (1985)
[51] Krinichnyi, V.I., Grinberg, O.Ya., Dubinsky, A.A., Livshits, V.A., Bobrov, Yu.A., Lebedev, Ya.S.: Biofizika 32, 534–535 (1987)
[52] Ingram, D.I.E.: Biological and Biochemical Application of Electron Spin Resonance, London: Adam.Ailder LTD 1969.
[53] Roth, H.K., Keller, F., Schneider, H.: Hochfrequenzspektroskopie in der Polymerforschung, Berlin: Akademie-Verlag 1984.
[54] Gordy, W., Kurita, Y.: J.Chem.Phys. 34, 282–288 (1960)
[55] Copeland, E.S.: J.Magn.Res. 20, 124–129 (1975)
[56] Krinichnyi, V.I., Shuvalov, V.F., Grinberg, O.Ya., Lebedev, Ya.S.: Khimich.Fizika (Russ) 1, 621–627 (1983)
[57] Dmitruk, A.F., Kholoimova, L.I., Krinichnyi, V.I., Grinberg, O.Ya., Shuvalov, V.F., Lebedev, Ya.S.: Khimich.Fizika (Russ) 5, 479–483 (1986)
[58] McCain, D.C., Palke, W.E.: J.Magn.Res. 20, 52–66 (1975)

Author's address: Dr.V.I.Krinichnyi, Department of Kinetic and Cathalysis, Institute of Chemical Physics of the Academy of Sciences of the USSR, Chernogolovka, 142432 USSR.